Bone 114 (2018) 235–245

Contents lists available at ScienceDirect

Bone

journal homepage: www.elsevier.com/locate/bone

Full Length Article

Iron overload involved in the enhancement of unloading-induced bone loss by hypomagnetic field

Jiancheng Yang[a,d,1], Xiaofeng Meng[c,1], Dandan Dong[a,d], Yanru Xue[a,d], Xin Chen[a,d], Shenghang Wang[a,d], Ying Shen[a,d], Gejing Zhang[a,d], Peng Shang[b,d,*]

[a] School of Life Sciences, Northwestern Polytechnical University, Xi'an 710072, China
[b] Research & Development Institute in Shenzhen, Northwestern Polytechnical University, Shenzhen 518057, China
[c] School of Food Science and Engineering, South China University of Technology, Guangzhou 510640, China
[d] Key Laboratory for Space Bioscience and Biotechnology, Institute of Special Environment Biophysics, Northwestern Polytechnical University, Xi'an 710072, China

ARTICLE INFO

Keywords:
Hypomagnetic field
Hindlimb unloading
Iron overload
Bone loss

ABSTRACT

During deep-space exploration missions, astronauts will be exposed to abnormal space environments including microgravity and hypomagnetic field (HyMF) that is 10,000 times weaker than geomagnetic field (GMF). It is well known that microgravity in space can induce bone loss; however, it is ill-defined whether HyMF involved in this process. Herein, we aimed to investigate the combined effects of HyMF and microgravity on bone loss. A mouse model of hindlimb suspension (HLU) was adopted to simulate microgravity-induced bone loss, that was exposed to a hypomagnetic field of < 300 nanotesla (nT) generated by a geomagnetic field-shielding chamber. Besides, a recent study showed that HLU induced bone loss was orchestrated by iron overload. Therefore, the changes of iron content in unloading-induced bone loss under HyMF condition were detected simultaneously. The results showed HyMF exacerbated the loss of bone mineral content (BMC), induced more detrimental effects on microstructure of cancellous bone but not cortical bone and yielded greater negative effects on biomechanical characteristics in mice femur under unloading status. Concomitantly, there was more iron accumulation in serum, liver, spleen and bone in the combined treatment group than in the separate unloading group or HyMF exposure group. These results showed that HyMF promoted additional bone loss in mice femur during mechanical unloading, and the potential mechanism may be involved in inducing iron overload of mice.

1. Introduction

In the history of biological evolution, all living organisms on the earth are exposed to the geomagnetic field (GMF) of about 50 microtesla (μT), a natural component of the habitable environment. However, the magnetic field (MF) in the space environment decreases geometrically with the distance from the ground. The MF magnitude (|B|) in the International Space Station is about 80% of GMF with limited variation [1]; but in outer space is extremely lower than the GMF, named a hypomagnetic field (HyMF, is defined by |B| < 5 μT), such as Martian MF is < 5 μT, Lunar MF is < 300 nT and interplanetary MF is just a few nanotesla [2]. Therefore, in addition to microgravity and cosmic radiation, astronauts must be exposed to the HyMF condition when onboard in the long-term and long-distance space missions.

Several experiments have clearly confirmed that the HyMF greatly disturbs many functional states of living organisms, including embryonic development, animal behaviors and brain function (reviewed in [3, 4]). In the cell level, shielding of the GMF inhibited growth rates of fibrosarcoma HT1080 and colorectal HCT116 cancer cells [5], decreased cell viability and mitochondrial activity in mouse skeletal muscle cell [6], stimulated the proliferation of mouse neural progenitor and stem cells [7] and accelerated the proliferation of human neuroblastoma cell [8]. The redox homeostasis ensures that the cells respond properly to endogenous and exogenous stimuli [9]. Elevated levels of cellular reactive oxygen species (ROS) were found in mouse skeletal muscle cell under a HyMF [6]. Lymphocytes from rats were exposed to HyMF for 15 min, 1 and 2 h, intracellular ROS levels were significantly reduced [10]. Low level magnetic fields suppressed H_2O_2 production in cancer cells and pulmonary artery endothelial cells [11]. Elimination of the GMF reduced hydrogen peroxide production in human neuroblastoma cell and inhibited the activity of CuZn superoxide dismutase [12]. However, there are limited reports about the effects of HyMF on bone cells. Bone is a constantly updated tissue, *i.e.*, bone remodeling, that happens throughout life to maintain a healthy skeleton. In the

* Corresponding author at: P.O. Box 707, 127 Youyi Xilu, Xi'an, Shaanxi 710072, China.
E-mail address: shangpeng@nwpu.edu.cn (P. Shang).
[1] Jiancheng Yang and Xiaofeng Meng equally contributed to this work.

https://doi.org/10.1016/j.bone.2018.06.012
Received 6 February 2018; Received in revised form 15 June 2018; Accepted 17 June 2018
Available online 19 June 2018
8756-3282/

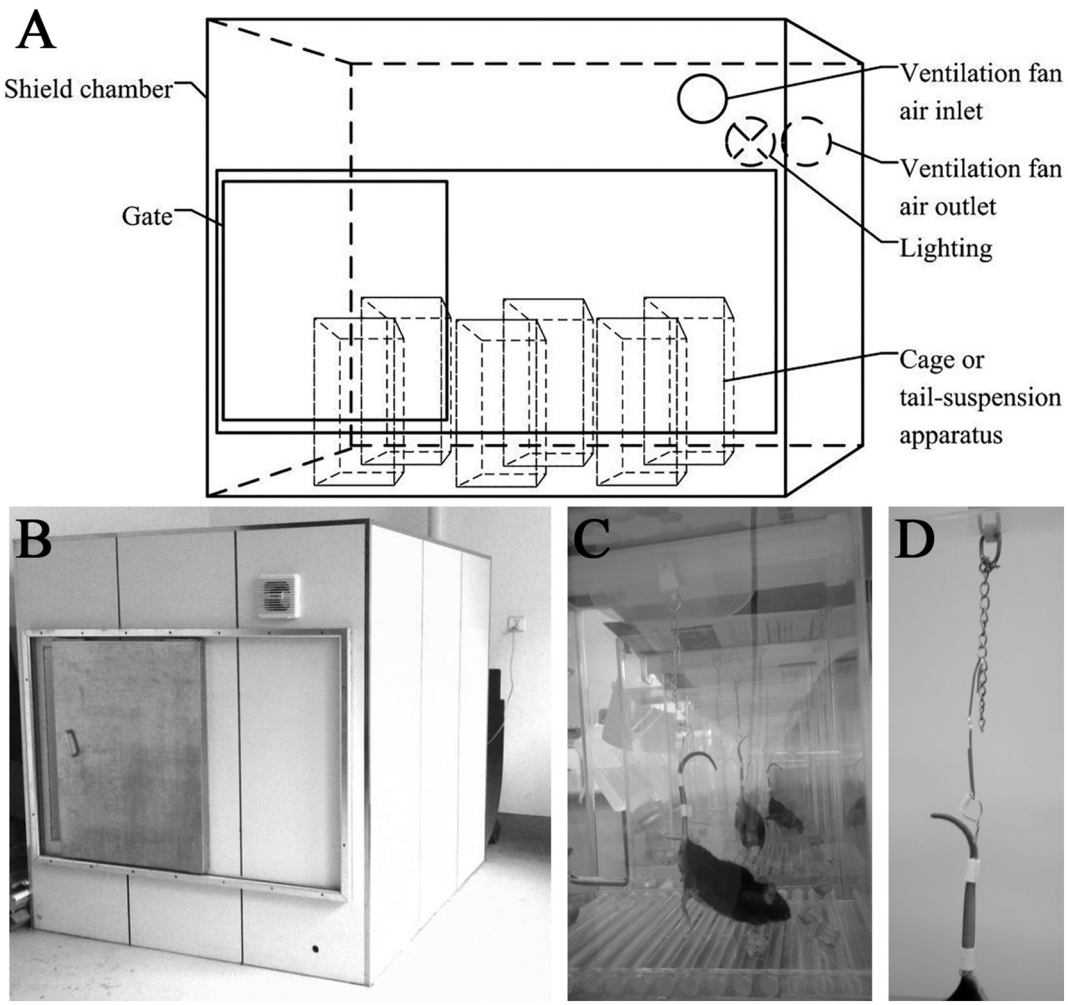

Fig. 1. Hypomagnetic environment experimental device. A) The schematic drawing of magnetic shielding chamber; B) Geomagnetic field shielding chamber; C) Mice under hindlimb unloading; D) A profile of tail-suspension.

course of bone remodeling, the old and damaged bone are removed by osteoclasts (bone resorption cells) and new bone is formed by osteoblasts (bone formation cells). Recently, we used a magnetic shielding box to create a hypomagnetic condition (~500 nT), performed a studies on the HyMF exposed murine osteoblasts MC3T3-E1 and found that there was no effect on cell proliferation; but HyMF exposure significantly inhibited the differentiation of osteoblasts by simultaneously retarding alkaline phosphatase (ALP) activity, mineralization and calcium deposition [13]. Moreover, we demonstrated that HyMF exposure significantly inhibited cell proliferation of pre-osteoclastic Raw264.7 cells and promoted osteoclasts differentiation, formation and bone resorption [14]. Although it has been established that the elimination of the GMF has adverse effects on living systems [15], HyMF effects on the skeletal system *in vivo* are unclear and have not been reported.

Bone loss has been thought to be the most important problem endangering the health of astronauts. There is a vast amount of data from spaceflight missions demonstrate that spaceflight induces a osteopenia in both humans and animals after prolonged stay in space [16]. Under environmental microgravity in space, increased calcium loss is observed in the skeletal system, especially from the weight-bearing bones; furthermore, incessant bone loss in astronauts may induce fractures and renal calculus, which may influence both their health and space missions [17]. Reduced mechanical stimulation is considered to be the main factor leading to bone loss in space. Spaceflight-induced bone loss has been proposed to be similar to disuse osteoporosis on Earth, which constitutes a challenging public health problem.

Iron is the essential metal element in the human body and play very important physiological and biochemical roles, including oxygen binding, electron transport, and serving as a catalyst for literally hundreds of enzymes [18]. However, iron is a highly transition metal and can catalyze the formation of hydroxyl radicals. As a consequence, the levels of iron beyond the tolerable threshold of cells can lead to a variety of adverse outcomes. Many evidence from *in vitro* experiments, animal models and clinical studies indicated that iron overload have direct detrimental effects on bone metabolism [19]. Excess iron inhibits the differentiation, proliferation, and activity of osteoblasts [20, 21], whereas it promotes osteoclast differentiation and bone-resorbing activity through the production of ROS *in vitro* [22, 23]. A murine model with treated high-dose iron dextran resulted in increased oxidative stress and bone resorption, leading to changes in bone remodeling and thus bone loss [24]. Case reports and clinical studies revealed that bone abnormalities appeared in patients with iron-loading conditions, such as hemoglobinopathies, hereditary hemochromatosis and menopause [19].

Evidence from space missions showed the changes in iron metabolism and hematology occur soon after entering microgravity, and a characteristic of this is a 10–15% decrease in red blood cell mass during flight because of neocytolysis [25]. One consequence of the reduced erythrocytes is the subsequent transfer of iron from those cells into storage proteins and processes. Evidence of this includes increased circulating levels of serum ferritin, an index of iron storage, after short- and long-duration space flight [26, 27]. In a recent long-duration

spaceflight, serum ferritin increased early, and transferrin and transferrin receptors decreased later, which indicated that the early increase in body iron stores generated through the mobilization of iron into storage tissues [28]. Higher iron stores are associated with higher levels of oxidative damage biomarkers, and with a greater degree of reduction in bone mineral density (BMD) after long-duration space flight [28]. There is a limited data on the physiological response to spaceflight due to the high cost. Thus a ground-based model of microgravity, hindlimb unloading (HLU) model, was developed by Morey-Holton et al. [29]. A recently study showed HLU induced bone loss in mice was associated with iron overload and coupled with the hepcidin which is the master regulator of iron homeostasis produced by the liver [30]. HLU in rats induced an increase of iron storage in the spleen and a decrease of circulating iron [31].

In summary, microgravity is one of the complex physical factors in space conditions, along with HyMF that should be carefully considered with regard to its effects on astronauts. Astronauts have acclimatized to the GMF, whereas HyMF is a novel environmental factor. It is unclear how the absence of the GMF and the presence of microgravity conditions influence the skeletal system health and the storage of body iron. In this study, a HLU model was utilized to simulate weightlessness and a permalloy magnetic shielding box designed for the realization of HyMF. We investigated the combined effects of a HyMF plus HLU on bone loss in male C57BL/6 mice and tried to understand the mechanism *via* iron metabolism.

2. Materials and methods

2.1. GMF-shielding chamber

A permalloy magnetic shielding chamber, 1.8 × 1.6 × 1.5 m, was used to create the HyMF environment (Fig. 1A, B). The magnetic field intensity was measured using a fluxgate magnetometer. The chamber can generate a HyMF environment with an average magnetic field intensity of < 300 nT. An additional ventilation system was fixed in the shielding chamber, with a ventilation frequency of 15 times per hour. The filament lamp was used for lighting inside the shielding chamber. The illumination switch was controlled with a 12-h light/12-h dark cycle. As a control, we constructed an experimental wooden box that has no shielding effect on GMF but has the same size, ventilation and illumination conditions as the GMF shielding chamber.

2.2. Animals procedures

We utilized male C57BL/6 mice (Charles River Laboratories, Beijing, China). Mice were 8 weeks old at day 0. Mice were fed with standard Rodent Diet (the Fourth Military Medical University, Xi'an, China) *ad libitum*, maintained at 25 °C, and kept on a 12 h light/dark cycle. One week before the experiment, mice were moved into the HLU enclosure to acclimatize new environment. Mice were weighed and then assigned to group to obtain an approximately equal average body weight per group. Experimental animals were divided into 4 group: (1) the control (Ctrl) group (n = 6) and (2) the HLU group (n = 8) in which mice were kept inside the wooden experimental box with the normal GMF environment; (3) the HyMF group (n = 6) and (4) the HyMF + HLU group (n = 8) in which mice were kept inside the GMF-shielding chamber.

The experiment lasted for 4 weeks. On day 28 of the experiment, the mice of all group were sent for a BMD scanning and blood samples were collected *via* cardiac puncture under anesthesia respectively. The mice were subsequently killed by luxating cervical vertebra under anesthesia status, and their bilateral femurs were separated from the soft tissues and immediately fixed in 4% paraformaldehyde for 2 days. The left femur was immersed in phosphate buffered saline and stored at 4 °C for micro-CT scanning. The right femur was decalcified with 10% EDTA solution and subsequently embedded in paraffin. The liver, spleen and duodenum of mice were separated and divided into two parts respectively. One part was fixed in 4% paraformaldehyde for 2 days and subsequently embedded in paraffin. Another part was weighed and stored at −80 °C. The animal protocol was approved by the Lab Animal Ethics and Welfare Committee, Northwestern Polytechnical University.

2.3. Hindlimb suspension model

At day 0, mice were subjected to tail-suspension in the HLU and the HyMF + HLU group. We utilized a HLU model described first by Morey-Holton et al. [29], with some minor improvements to the fixation of the mice tails (Fig. 1C, D). Briefly, one side in two strips of medical tape was wrapped around the tail in bottom and one-third location, another side was fixed to a copper wire ring attached to the tail tightly. A paper clip was straightened and connected with the copper wire ring at one end, opposite end was hung in a stainless steel chain with a swivel hook. The swivel hook was wound around the cross bar at the top of the cage. The hindquarters of the animal were raised or lowered to achieve a 30° elevation. This angle of suspension has been previously demonstrated to keep the forelimbs normally-loaded, while minimizing tail tension and animal stress [32]. Control mice were housed in the same cage as HLU group, though without attachment of the tail-suspension apparatus. Animal appearance, responsiveness and mobility were assessed daily. In the first few days of HLU, special concern should be taken to prevent urethral crusting and potential infections in male mice. The urethra was cleaned with sterile gauze and warm 0.9% sterile saline as necessary.

2.4. In vivo dual-energy X-ray absorptiometry (DXA)

Dual-energy X-ray absorptiometry (DXA) (InAlyzer; MEDIKORS, Korea) in the small-animal model was used to measure BMD and BMC of whole femurs *in vivo*. On day 28 of the experiment, all experimental animals were anesthetized and placed in the absorptiometry machine for BMD and BMC measurement. The scanning results were analyzed with a dual X-ray digital imaging software (InAlyzer; MEDIKORS, Korea) for assessing the BMD and BMC of whole bilateral femurs.

2.5. Micro-computed tomography

Left femurs were scanned using a micro-CT scanner (SkyScan 1176; Bruker, Kontich, Belgium). Scanning was performed at 80 kV, 305 mA, 525 ms without filter. In total, 421 projections were collected per sample at a resolution of 8.96 μm per pixel. Three-dimensional reconstruction and analyses of the samples were performed using NRecon and CTAn software, respectively (Bruker). The area-of-interest (ROI) was selected employing an automated algorithm. Two 1-mm-long ROI were selected for analysis of trabecular bone (distance from the distal growth plate 0.5 mm to 1.5 mm) and cortical bone (distance from the distal growth plate 0.5 mm to 1.5 mm). Parameters are reported according to published guidelines [33]. Trabecular parameters included bone volume fraction (BV/TV), thickness (Tb.Th), separation (Tb.Sp), number (Tb.N), connectivity density (Conn.D) and structure model index (SMI). Cortical parameters included cortical area (Ct.Ar), total area (Tt.Ar), marrow area (Ma.Ar), cortical thickness (Ct.Th), cortical porosity (Ct.Po) and polar moment of inertia (PMOI).

2.6. Biomechanical testing

After MicroCT scanning, left femurs were mechanically tested to failure *via* three-point bending using a Bose testing apparatus (Bose Corporation, ElectroForce BioDynamic, ELF3200; USA). Flexural support spans were 8 mm. A loading rate of 0.02 mm/s was applied in the medial to lateral direction until the femur fractured. Displacement and force were used to calculate parameters describing whole bone structural properties. The maximum load (F_{max}, breaking load) was

transformed to the ultimate bending moment ($M = F_{max}L/4$), where L = span length of 8 mm. Using the software of the material testing machine, the stiffness (K) as the tangent modulus of the linear part of the force-displacement curve [34]. The elastic modulus (E) and ultimate stress (S) was calculated by equations, $E = KL^3/(48I)$ and $S = F_{max}Lc/(4I)$ [35], where I (moment of inertia) and c (distance from centroid of cross-section to outermost point on the cross-section) from the analysis of CTAn software.

2.7. Biochemical assay

The blood samples were centrifuged (3000 rpm; 15 min; 4 °C), serum was fractionated and stored in a −80 °C freezer. Serum ferritin, hepcidin, alkaline phosphatase (ALP) and tartrate-resistant acid phosphatase 5b (TRAP5b) were measured by using a mouse enzyme linked immunosorbent assay (ELISA) kit (Shanghai Jianglai Biotech, Shanghai, China). All steps followed the manufacturer's instructions.

2.8. Iron measurements

The total iron content in the left femur, liver, spleen and duodenum was detected by atomic absorption spectroscopy (AAS; Analytik Jena, Germany). Tissue weight was determined and placed in a porcelain crucible. Samples were dried at 110 °C overnight, dry weight was determined. Afterwards, they were ashed in a resistance furnace (TAISITE, Tianjin, China) at 550 °C. The ash was dissolved in 65% spectra pure HNO3, and its total iron level was determined by atomic absorption. Iron content was normalized by dry weight of bone.

2.9. Histological analysis

After the paraffin embedding, right femur, liver, spleen and duodenum were sectioned at 5 μm *via* a semi-automated rotary microtome (Leica Biosystems RM2245, Germany). To visualize ferric iron deposits, slides were stained with Prussian Blue (Sigma-Aldrich, USA) followed by a 20 min incubation with DAB (Sigma-Aldrich, USA). Meyer's hematoxylin was used as counterstain.

To evaluate bone formation and bone resorption, osteoblasts and osteoclasts in the cancellous bone of the distal femur were counted. Osteoblasts were showed by morphology in sections stained with hematoxylin and eosin (H&E; Beyotime Biotechnology, Shanghai, China) according to standard procedures; osteoclasts were displayed by TRAP staining using a commercially TRAP kit (Sigma-Aldrich, USA) followed by counterstaining with Gills Hematoxylin (Sigma) [36]. Images were analyzed by Image J software (National Institutes of Health, USA).

2.10. Statistical analysis

Data are presented as mean ± standard error. We used two-way ANOVA with Sidak's multiple comparisons test when the interaction had significant differences. P values of < 0.05 were regarded as significant. All statistical analysis was performed using the Prism software (Graphpad prism for Windows, version 6.01).

3. Results

3.1. Hypomagnetic field aggravates bone loss in femurs of hindlimb unloaded mice

To investigate the effects of HyMF on bone loss in hindlimb unloaded mice, the BMD and BMC, mechanical properties and microarchitecture of femur were analyzed. DXA analysis showed that the femoral BMD and BMC were significantly decreased in the HLU and HyMF + HLU group compared to the control and HyMF group (Fig. 2A, B). The differences in BMD and BMC of femur were not significant between the HyMF and control group. The femoral BMC was lower in the HyMF + HLU group than in the HLU group, whereas no significant difference in the BMD of femur (Fig. 2A, B).

The three-point bending test showed the ultimate bending moment, elastic modulus, stiffness and ultimate stress of femur in the HLU and HyMF + HLU group were significantly lower than the control and HyMF group (Fig. 3). HyMF had no any effect on mechanical properties of mice femur. The HyMF + HLU group has lower mean value in ultimate bending moment and ultimate stress significantly than in the HyMF and HLU group (Fig. 3A, D).

Most trabecular parameters of the proximal femur including BV/TV, Tb.Sp, Tb.N, Conn.Dn and SMI, and most cortical parameters of femoral shaft including Ct.Ar, Ma.Ar, Ct.Th and Ct.Po did significant change in the HLU and HyMF + HLU group compared with that of the control group. All microstructure parameters of femur were not difference in HyMF *vs.* Control. Suspended mice in the HyMF condition had lower BV/TV and Conn.Dn and higher Tb.Sp than the GMF condition (Fig. 4B). However, there were non-significant changes in all cortical bone parameters between the HLU and HyMF + HLU group (Fig. 4D). Representative three-dimensional images of femoral trabecular and cortical bone in each group were displayed in Fig. 4A and C.

3.2. Effects of hypomagnetic field on bone remodeling in femurs of hindlimb unloaded mice

Hindlimb unloading-induced bone loss is accompanied by reduced osteoblast activity and increased osteoclast activity [37]. To assess bone loss in HLU model under HyMF condition, we analyzed the changes in osteoblast and osteoclast activity. Histological examination of the distal femoral trabecular bone revealed the changes of osteoblasts and osteoclasts and ELISA assay detected the changes of bone formation marker and bone resorption marker. The number of osteoblasts was decreased (Fig. 5A, B), accompany with decreased ALP concentration of serum in the HLU group and HyMF + HLU group (Fig. 5C). Oppositely, the amount of TRAP-positive osteoclasts was increased (Fig. 5D, E), accompany with increased TRAP5b concentration of serum in the HLU group and HyMF + HLU group (Fig. 5F). There was not any difference between the HyMF group and the control group in either the number of osteoblasts and osteoclasts or ALP and TRAP5b level in serum (Fig. 5). In the HyMF + HLU group, more osteoclasts and fewer osteoblasts were observed in femur than in HLU mice under GMF. Osteoclasts in unloaded mice under HyMF secreted more TRAP5b into the serum than in separate HLU treated mice. No differences were detected between the HLU group and the HyMF + HLU group in serum ALP level.

3.3. Hypomagnetic field increases body iron store in hindlimb unloaded mice

To reveal the effects of HyMF on body iron accumulation in hindlimb unloaded mice, iron levels in serum, liver, spleen and duodenum were detected. As showed in Fig. 6A and B, serum iron and ferritin content in the HLU and HyMF + HLU group were significantly higher than the control and HyMF group. Serum iron and ferritin level in the HyMF group were similar to the control. Compared to the HLU group, the levels of serum iron and ferritin increased markedly in the HyMF + HLU group. It is well known that serum hepcidin that is a key regulator of iron metabolism in mammals [38]. Compared with the control and HyMF group, higher serum hepcidin concentration was found in the HLU and HyMF + HLU group. There was no statistical difference between the HLU group and the HyMF + HLU group (Fig. 6C).

DAB-enhanced Perls' iron staining indicated that iron was conspicuously deposited in the liver (Fig. 7A) and spleen (Fig. 7C) for the HLU and HyMF + HLU group, this could also be observed through their iron content, respectively (Fig. 7B, D). No significant differences were observed for iron accumulation of the liver and spleen in the HyMF and control group. Compared to the HLU group, iron deposition in the liver

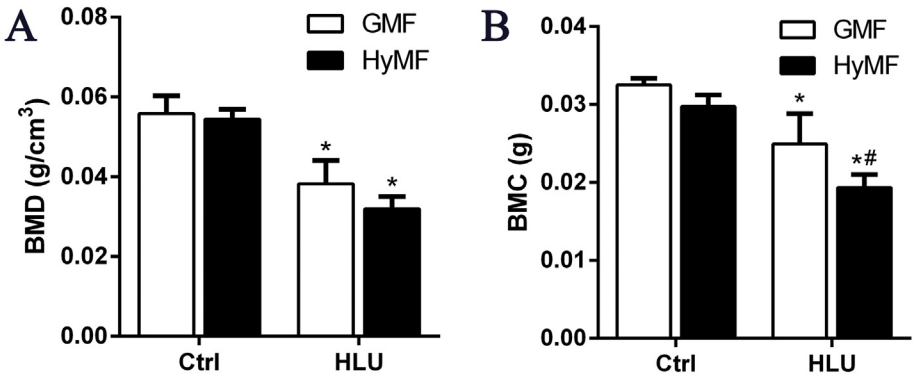

Fig. 2. The effects of HyMF and HyMF + HLU on femoral BMD and BMC. DXA analysis of whole femoral bone mineral density (BMD, A) and bone mineral content (BMC, B). Ctrl: Mice were kept in a wooden experimental box with the normal GMF for 28 days; HLU: Mice were suspended and raised in a wooden box; HyMF: Mice were raised normally in a GMF-shielded room; HyMF + HLU: HLU mice were raised in a GMF-shielded room (n = 6–8/group). Data shown as Mean ± SD. $^{*}P < 0.05$ *vs.* Ctrl, $^{\#}P < 0.05$ *vs.* HyMF.

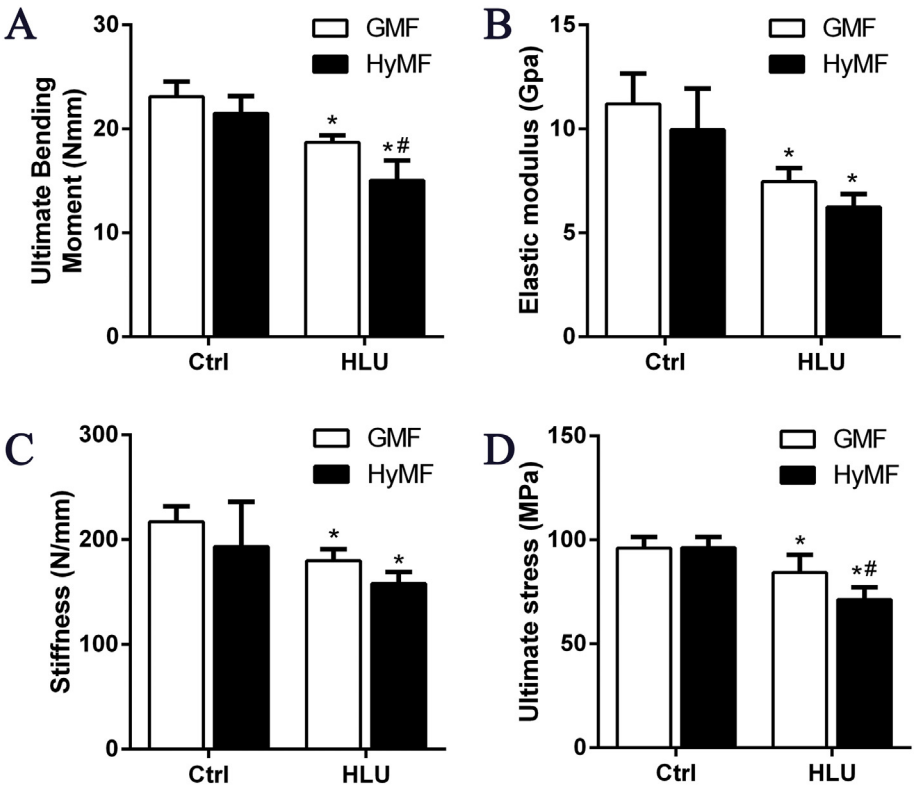

Fig. 3. The Effects of HyMF and HyMF + HLU on the mechanical properties of femur in mice. Ultimate bending moment (A), elastic modulus, (B) Stiffness (C) and Ultimate stress (D) were calculated by using the raw data 3-point bending. Ctrl: Mice were kept in a wooden experimental box with the normal GMF for 28 days; HLU: Mice were suspended and raised in a wooden box; HyMF: Mice were raised normally in a GMF-shielded room; HyMF + HLU: HLU mice were raised in a GMF-shielded room (n = 6–8/group). Data shown as Mean ± SD. $^{*}P < 0.05$ *vs.* Ctrl, $^{\#}P < 0.05$ *vs.* HyMF.

and spleen were more severe in the HyMF + HLU group by observing their histologic staining and analyzing their iron content, respectively (Fig. 7A–D). In duodenum, there were no any changes between the four groups (Fig. 7E, F).

Taken together, these results suggest that hindlimb unloading-induced iron store increase in liver and spleen was enhanced by HyMF condition.

3.4. Hypomagnetic field aggravates iron overload in femurs of hindlimb unloaded mice

Iron overload is closely associated with bone loss. Thus iron contents in femur and bone marrow were examined. The results showed that iron contents of femur and bone marrow were markedly increased in the HLU and HyMF + HLU group compared with the control and HyMF group (Fig. 8A, B). The differences of iron content in femur and bone marrow were not significant between the HyMF and control group. Compared to the HLU group, iron level of femur and bone marrow in the HyMF + HLU group was significant increase. Correspondingly, the iron deposition in bone marrow could be observed from the section of femoral cancellous bone and cortical bone with DAB-enhanced Perls blue staining (Fig. 8C, D).

4. Discussion

In this study, we assessed the combined effect of HLU model and HyMF condition on bone homeostasis in mice and tried to understand the potential mechanism *via* iron metabolism. The results showed that HyMF aggravated the loss of BMC; induced more deleterious effects on microstructure of cancellous bone, including BV/TV, Tb.Sp and Conn.Dn; and yielded greater negative effects on biomechanical characteristics, such as ultimate bending moment and ultimate stress in mice femur under unloading status. Concomitantly, there was more iron accumulation in serum, liver, spleen and bone in the combined treatment group than in the separately unloaded group or HyMF exposure group. These data showed that HyMF promoted additional bone loss in simulated weightlessness, and the potential mechanism may be involved in inducing iron overload of mice.

HyMF is an environmental factor of outer space, and is far weaker than the GMF. Organisms on Earth might have accommodated the presence of GMF in a billion-year evolution. Elimination of GMF may affect organisms. HyMF has been suggested to influence negatively on

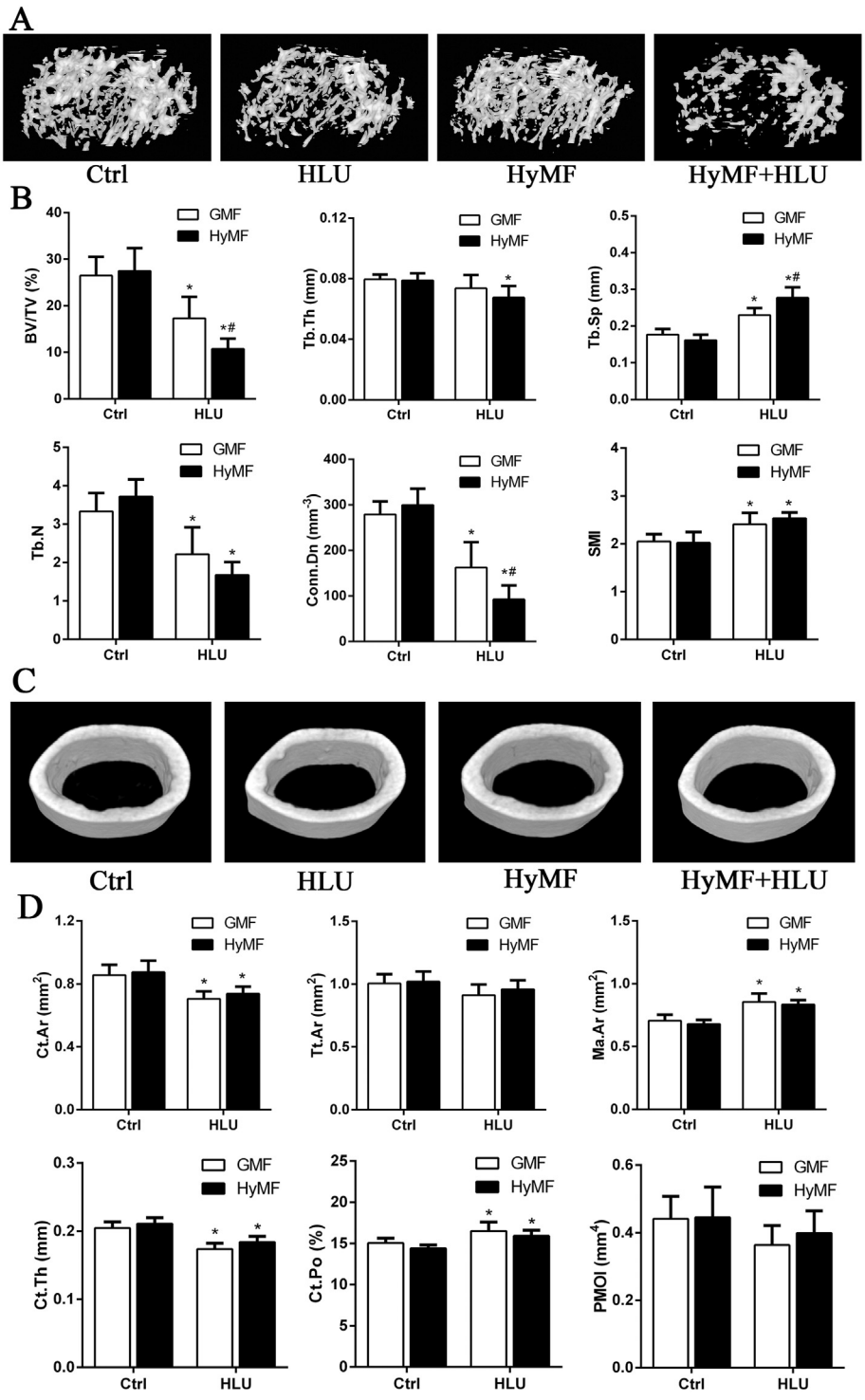

Fig. 4. Effects of HyMF and HyMF + HLU on trabecular and cortical microstructure parameters of femurs in mice. Trabecular and cortical microstructure parameters obtained *via* microcomputed tomography scans. (A) Three-dimensional trabecular architecture of an ROI located in 0.5 mm proximal to the distal growth plate. (B) Measured parameters at the distal femur, including bone volume fraction (BV/TV), trabecular thickness (Tb.Th), trabecular separation (Tb.Sp), trabecular number (Tb.N), connectivity density (Conn.D), structure model index (SMI). (C) Three-dimensional cortical architecture of an ROI located in 5 mm proximal to the distal growth plate. (D) Measured parameters at the midshaft femur, including cortical area (Ct.Ar), total area (Tt.Ar), marrow area (Ma.Ar), cortical thickness (Ct.Th), cortical porosity (Ct.Po), polar moment of inertia (PMOI). Ctrl: Mice were kept in a wooden experimental box with the normal GMF for 28 days; HLU: Mice were suspended and raised in a wooden box; HyMF: Mice were raised normally in a GMF-shielded room; HyMF + HLU: HLU mice were raised in a GMF-shielded room (n = 6–8/group). Data shown as Mean ± SD. $^{*}P < 0.05$ *vs.* Ctrl, $^{\#}P < 0.05$ *vs.* HyMF.

the early embryonic development [39, 40] and the function of the central nervous system [41, 42]. However, HyMF effects on the skeletal system are unclear and have not been reported. In this study, male C57BL/6 mice with 8 weeks old were exposed to HyMF for 28 days. We found that HyMF exposure does not cause a deleterious effect on femur of mice. However, our two *in vitro* experiments found that HyMF exposure significantly inhibited the differentiation of osteoblasts [13] and promoted osteoclastic formation and bone absorption function [14]. These seemingly contradictory findings can be attributed to the differences of environment and characteristic between *in vitro* and *in vivo* cells. This also reminds us that *in vitro* study requires the examination *in vivo*.

Humans in space are at high risk for bone loss. At present, it is widely accepted that microgravity plays a predominant role in bone homeostasis disorders in spaceflight [17]. However, except for microgravity, there are many other extreme environments in space, such as hypomagnetic fields (HyMF), radiation, *etc.* are different from the ground. These conditions, which act simultaneously, resulted in many physical health problems of space travelers in space [43]. HLU induces bone loss similar to those data from spaceflight and can be considered a relatively accurate approximation of exposure to real weightlessness for the unloaded limbs [37]. So far, the combined effects between radiation

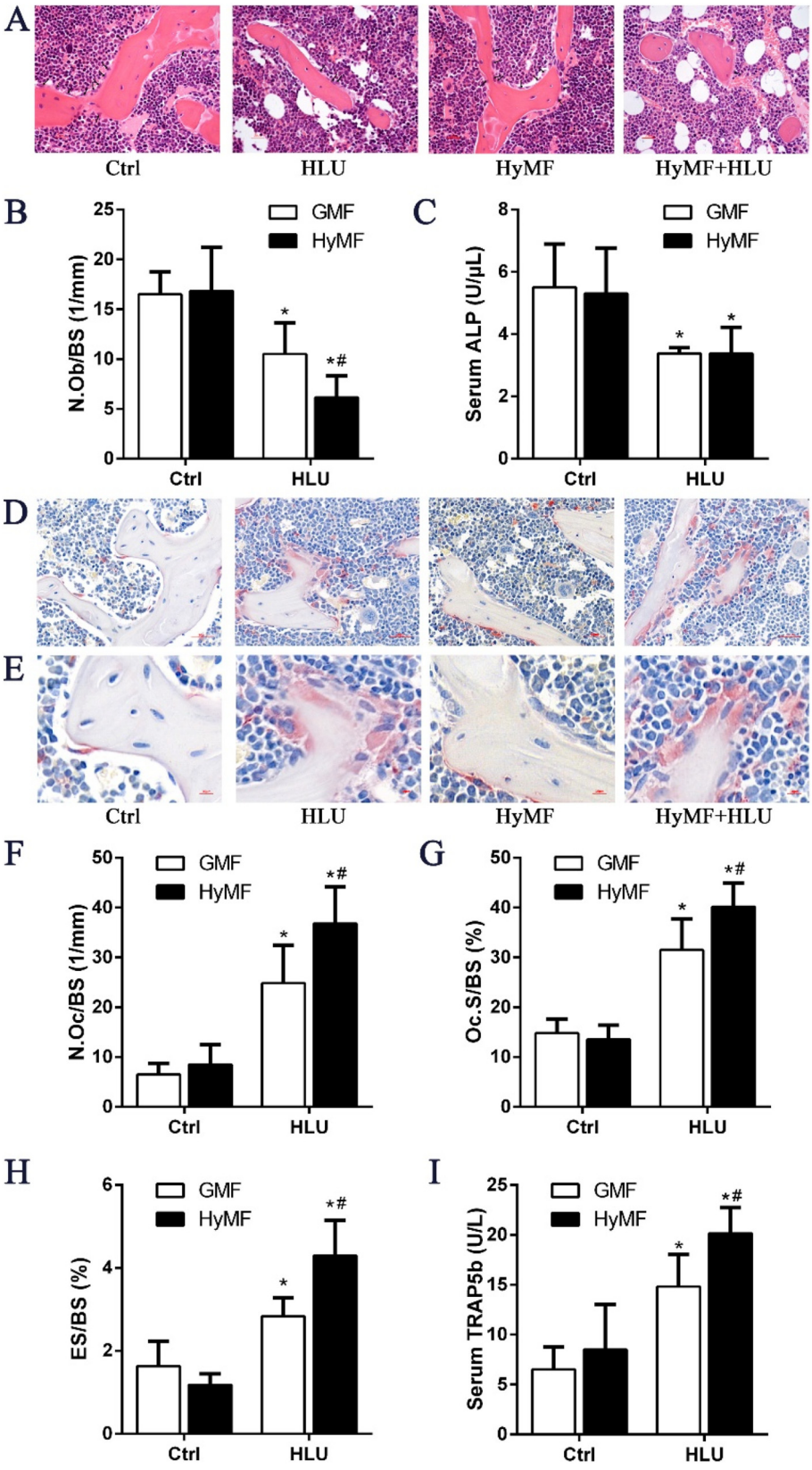

Fig. 5. Effects of HyMF and HyMF + HLU on bone formation and bone resorption of femurs in mice. A) Hematoxylin and Eosin (H&E) staining of trabecular bone on the distal of femur and osteoblasts were marked in black arrow (Bar = 20 μm); B) The number of osteoblasts were evaluated by osteoblast number per bone surface (N.Ob/BS); C) Serum levels of the bone formation markers alkaline phosphatase (ALP); TRAP staining of trabecular bone on the distal of femur and osteoclasts were identified on the bone surfaces by red TRAP staining (D, Bar = 50 μm; E, Bar = 10 μm); F) The number of osteoclasts were evaluated by osteoclast number per bone surface (N.Oc/BS); G) The osteoclast surface per bone surface (Oc.S/BS); H) The eroded surface per bone surface (ES/BS); I) Serum levels of tartrate resistant acid phosphatase (TRAP5b) were evaluated as markers of bone resorption. Ctrl: Mice were kept in a wooden experimental box with the normal GMF for 28 days; HLU: Mice were suspended and raised in a wooden box; HyMF: Mice were raised normally in a GMF-shielded room; HyMF + HLU: HLU mice were raised in a GMF-shielded room (n = 6–8/group). Data shown as Mean ± SD. $^{*}P < 0.05$ *vs.* Ctrl, $^{\#}P < 0.05$ *vs.* HyMF.

and simulated microgravity on bone have been investigated in numerous studies [44–46], while the interaction of HyMF with microgravity on bone has not drawn enough attention. Therefore, the interaction effect of microgravity and HyMF on bone was evaluated in this study. We used a HLU model of mice, that was exposed to a HyMF condition of < 300 nT generated by a geomagnetic field-shielding chamber. The results indicated that BMC, BV/TV, Conn.Dn, ultimate bending moment and ultimate stress of femur were dramatically decreased in the HLU and HyMF + HLU group compared with the control and HyMF group. Moreover, these parameters were significantly lower

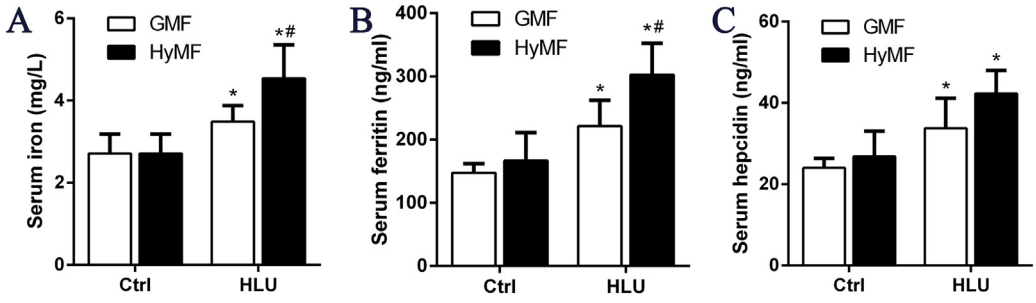

Fig. 6. Effects of HyMF and HyMF + HLU on iron, ferritin and hepcidin levels in serum of mice. The level of serum iron (A), ferritin (B) and hepcidin (B) were calculated by using mouse ELISA kits. Ctrl: Mice were kept in a wooden experimental box with the normal GMF for 28 days; HLU: Mice were suspended and raised in a wooden box; HyMF: Mice were raised normally in a GMF-shielded room; HyMF + HLU: HLU mice were raised in a GMF-shielded room (n = 6–8/group). Data shown as Mean ± SD. $^{*}P < 0.05$ *vs.* Ctrl, $^{\#}P < 0.05$ *vs.* HyMF.

in the HyMF + HLU group than in the HLU group. However, interestingly enough, HyMF by itself had no impact on any variable measured in this study. A plausible explanation is that HyMF effects are so weak that bone homeostasis cannot be broken. While bone homeostasis becomes disordered in unloading condition, the detrimental effects of HyMF on bone may be magnified.

Ferritin is an iron storage protein, already as an index of iron stores for clinical evaluation [47]. Although many indexes are available, determination of iron status by using serum ferritin (SF) concentrations is the most efficient indicators used in clinical and public health settings [48]. Evidence from short- and long-duration spaceflights showed that astronauts had increased levels of circulating SF [26, 27]. A recent long-duration spaceflight with 23 cosmonauts, SF levels increased about 220% in women and 70% in men by flight day 15 [28]. Furthermore, higher SF stores connected with a greater degree of reduction in BMD of the hip, trochanter, hip neck, and pelvis after long-duration spaceflight [28]. As a simulated microgravity model, we found an increased level of serum iron and ferritin in mice subjected to HLU or HLU + HyMF for 28 days. Concomitantly, DXA analysis showed that the femoral BMD were significantly decreased in the HLU and HyMF + HLU group compared to the control and HyMF group. These data are important to show that SF concentrations were probably associated with osteopenia in mechanical unloading.

A majority of the redundant body iron is found in hepatocytes and reticuloendothelial macrophages, which serve as a repository of iron [49]. The liver can easily take up an amount of circulating iron that exceeds the binding capacity of plasma transferrin [50]. HLU has been showed can induce an increased iron content and ferritin level in liver of mice [30]. Similarly, our study also demonstrated that elevated iron deposit of liver was observed by the Prussian blue staining in mice with HLU treating. Moreover, more iron accumulation presented in liver of mice which were subjected to HLU under GMF or HyMF condition. Spleen contains a large number of macrophages, senescent or other aberrant erythrocytes are normally phagocytosed by macrophages, followed by degradation of their hemoglobin [51]. The most dramatic increase in the amount and distribution of iron in HLU and HyMF + HLU treated mice occurred in the spleen. This is probable a result that erythrophagocytosis of damaged red blood cells were increased in spleen of unloaded mice. Indeed, report from space missions showed a 10–15% decrease in red blood cell mass during flight because

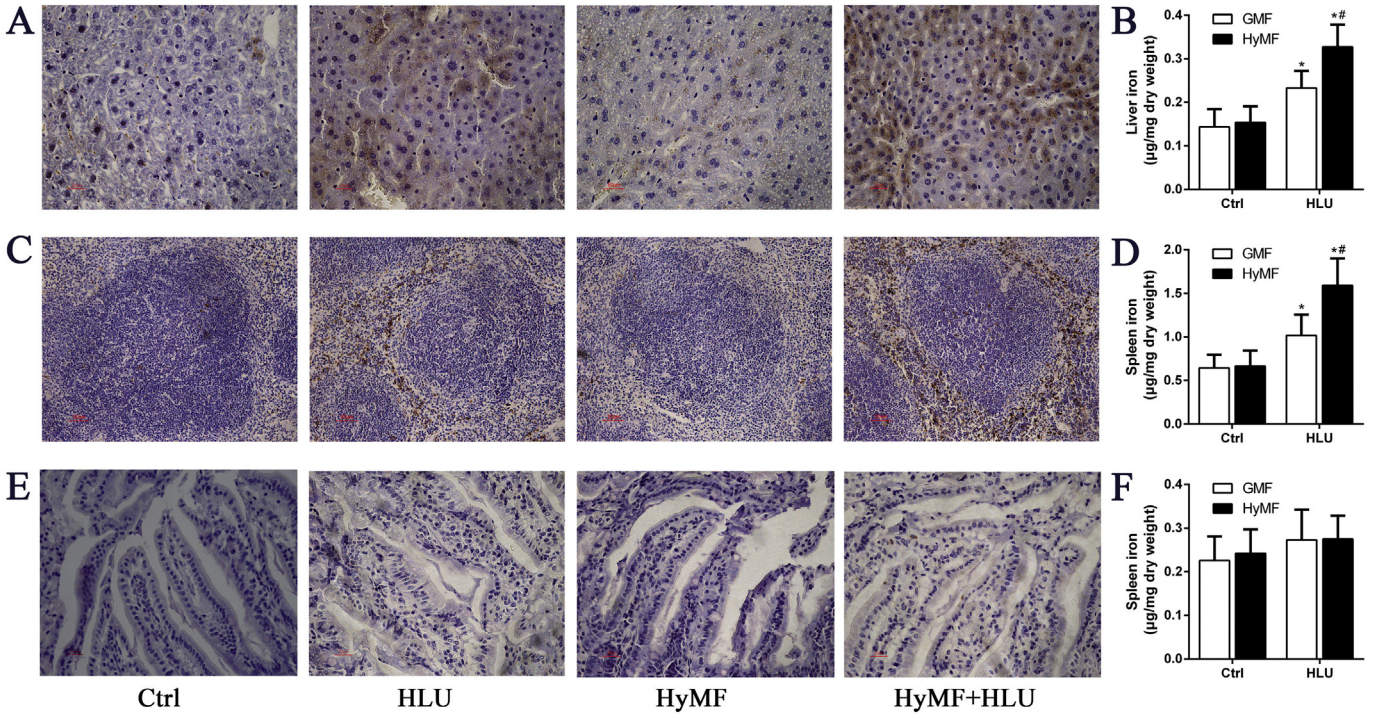

Fig. 7. Effects of HyMF and HyMF + HLU on iron distribution in tissues of mice. Histological analysis of iron deposits in liver (A, Bar = 20 μm), spleen (C, Bar = 50 μm) and duodenum (E, Bar = 20 μm) sections by Perls' iron staining. Atomic absorption spectrometry detected the total iron content in liver (B), spleen (D) and duodenum (F). Ctrl: Mice were kept in a wooden experimental box with the normal GMF for 28 days; HLU: Mice were suspended and raised in a wooden box; HyMF: Mice were raised normally in a GMF-shielded room; HyMF + HLU: HLU mice were raised in a GMF-shielded room (n = 6–8/group). Data shown as Mean ± SD. $^{*}P < 0.05$ *vs.* Ctrl, $^{\#}P < 0.05$ *vs.* HyMF.

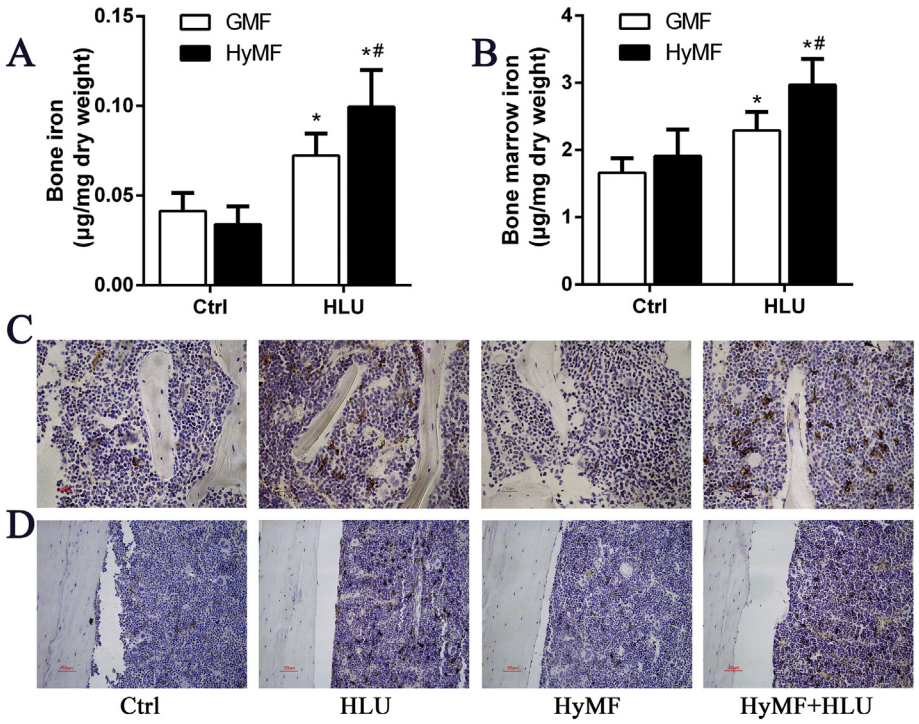

Fig. 8. Effects of HyMF and HyMF + HLU on iron content in femurs of mice. The total iron content in diaphysis (A) and bone marrow (B) of femur was detected by AAS. DAB-enhanced Perls' iron staining in cancellous bone (C, Bar = 20 μm) and cortical bone (D, Bar = 50 μm) of femur. Ctrl: Mice were kept in a wooden experimental box with the normal GMF for 28 days; HLU: Mice were suspended and raised in a wooden box; HyMF: Mice were raised normally in a GMF-shielded room; HyMF + HLU: HLU mice were raised in a GMF-shielded room (n = 6–8/group). Data shown as Mean ± SD. $^{*}P < 0.05$ *vs.* Ctrl, $^{\#}P < 0.05$ *vs.* HyMF.

of neocytolysis [25]. The iron from the reduced erythrocytes is transferred into storage tissues and circulation.

Hepcidin is the master regulator of iron homeostasis and ferroportin is an iron exporter present on the surface of enterocytes, hepatocytes and macrophages [38]. After binding to hepcidin, ferroportin is internalized and degraded, leading to decreased export of cellular iron [38]. In the current study, we demonstrated that serum hepcidin concentrations were elevated in unloaded mice under GMF and HyMF condition. Although there was no statistical difference between the HLU group and the HyMF + HLU group, upward hepcidin level could be found when shielding the geomagnetic field, and accompanied by iron overload in liver, spleen and bone. Hepcidin is a peptide hormone secreted by the liver. Although the expression of hepcidin was not determined in this study, a recent study demonstrated hepcidin expression of liver in male C57BL/6 mice was upregulated during unloading [30]. Moreover, HLU induced hepcidin upregulation through the inflammatory signaling pathway IL-6/STAT3 but not BMP/SMAD pathway in male Wistar rats [31]. Interestingly, iron overload driven bone loss was associated with increased production of inflammatory cytokines such as tumor necrosis factor-α (TNF-α) and interleukin-6 (IL-6) [24]. In conclusion, it is possible that the increase of hepcidin expression during unloading in response to iron loading and inflammation.

Iron catalyzes the formation of reactive oxygen species (ROS) is found to be critical in iron-mediated osteoblast activity and osteoclast activity. Iron overload probably inhibited osteoblast activity through higher oxidative stress following increased intracellular iron concentrations [52]. Ferric ion could promote RANKL-induced osteoclast differentiation and bone resorption through the production of ROS [22]. Iron overload induced bone loss in mice was associated with increased production of ROS, and the free radical scavenger *N*-acetyl-L-cysteine (NAC) could partially prevent the development of bone deformities caused by excess iron [24]. Importantly, numerous experiments from spaceflight and ground-based models have revealed that skeletal responses to spaceflight are related to redox signaling and oxidative stress [53]. A study in a long duration on the International Space Station, was performed to evaluate the association of iron status with oxidative damage and bone loss in astronauts [28]. The results showed the changes of SF were definitely correlated with the oxidative damage markers, suggesting that elevated iron storage during spaceflight might be a risk factor for oxidative damage and bone resorption [28]. Moreover, intracellular ROS generation induced by mechanical unloading, contributed to the occurrence of bone loss [54]. In our study, we demonstrated that increased iron store was found in the HLU group, and HyMF accelerated more iron accumulation and bone loss in unloaded mice. Therefore, it is a hypothesis that higher oxidative stress induced by iron overload is a cause of the enhancement of unloading-induced bone loss by HyMF.

Bone formation by osteoblasts, and bone resorption by osteoclasts, are tightly coupled to maintain bone homeostasis, namely bone remodeling [55]. Astronauts showed a trend toward decreased bone formation markers and increased bone resorption markers [56, 57]. Similar to the observation from several study using tail suspension in C57BL/6 mice [30, 58, 59]. Here we found a moderate decrease in bone formation and a dramatic increase in bone resorption after 28 days of unloading in C57BL/6 mice. Furthermore, increasing evidence indicates that both increased bone resorption by osteoclasts and decreased bone formation by osteoblasts are concerned in the pathological osteoporosis in iron overload conditions [19]. Osteoblasts are derived from the differentiation of bone marrow mesenchymal stem cells (BMSCs) and osteoclasts differentiate from the bone marrow monocyte/macrophage hematopoietic lineage [55]. Balogh et al. [21] showed that iron selectively inhibits osteogenic differentiation of BMSCs without influencing adipogenic and chondrogenic differentiation. On the other hand, a study suggested that the biological functions of monocytes/macrophages need moderate iron, while osteoclasts require a high level of iron [60]. Importantly, our results showed the iron content of femoral bone marrow was increased, accompany with decreased amount of osteoblasts and increased number of osteoclasts in femur of unloaded mice. Moreover, in unloaded mice under HyMF, there were more iron level in femoral bone marrow, more osteoclasts and less osteoblasts were observed in femur than in HLU mice under GMF. Therefore, iron overload may be involved in HyMF aggravated bone loss in unloading by decreased bone formation and increased bone resorption.

In summary, we demonstrated that HyMF can promote additional bone loss in hindlimb unloading-induced bone loss in male C57BL/6 mice. The underlying mechanism might involve in the increase of body

iron storage, which may induce oxidative stress responses. This study introduces an influence factor, HyMF, for spaceflight induced bone loss. Moreover, these findings provide a potential prevention strategy for space induced osteoporosis, by exposing astronauts to a certain intensity of the magnetic field or targeting the iron metabolism pathway.

Declaration of interest

The authors report no conflicts of interest. The authors alone are responsible for the content and writing of the paper.

Acknowledgments

This work sponsored by the Innovation Foundation for Doctor Dissertation of Northwestern Polytechnical University (CX201839) and the National Natural Science Foundation of China (51477141 and 51777171).

References

[1] C. Del Seppia, L. Mezzasalma, M. Messerotti, A. Cordelli, S. Ghione, Simulation of the geomagnetic field experienced by the International Space Station in its revolution around the Earth: effects on psychophysiological responses to affective picture viewing, Neurosci. Lett. 400 (3) (2006) 197–202.
[2] W.C. Mo, Y. Liu, R.Q. He, A biological perspective of the hypomagnetic field: from definition towards mechanism, Prog. Biochem. Biophys. 39 (9) (2012) 835–842.
[3] W. Mo, Y. Liu, R. He, Hypomagnetic field, an ignorable environmental factor in space? Sci. China Life Sci. 57 (7) (2014) 726–728.
[4] V.N. Binhi, F.S. Prato, Biological effects of the hypomagnetic field: an analytical review of experiments and theories, PLoS One 12 (6) (2017) e0179340.
[5] C.F. Martino, L. Portelli, K. McCabe, M. Hernandez, F. Barnes, Reduction of the Earth's magnetic field inhibits growth rates of model cancer cell lines, Bioelectromagnetics 31 (8) (2010) 649–655.
[6] J.P. Fu, W.C. Mo, Y. Liu, R.Q. He, Decline of cell viability and mitochondrial activity in mouse skeletal muscle cell in a hypomagnetic field, Bioelectromagnetics 37 (4) (2016) 212–222.
[7] J.P. Fu, W.C. Mo, Y. Liu, P.F. Bartlett, R.Q. He, Elimination of the geomagnetic field stimulates the proliferation of mouse neural progenitor and stem cells, Protein Cell 7 (9) (2016) 624–637.
[8] W.C. Mo, Z.J. Zhang, Y. Liu, P.F. Bartlett, R.Q. He, Magnetic shielding accelerates the proliferation of human neuroblastoma cell by promoting G1-phase progression, PLoS One 8 (1) (2013) e54775.
[9] D. Trachootham, W. Lu, M.A. Ogasawara, N.R.-D. Valle, P. Huang, Redox regulation of cell survival, Antioxid. Redox Signal. 10 (8) (2008) 1343–1374.
[10] P. Politanski, E. Rajkowska, M. Brodecki, A. Bednarek, M. Zmyslony, Combined effect of X-ray radiation and static magnetic fields on reactive oxygen species in rat lymphocytes in vitro, Bioelectromagnetics 34 (4) (2013) 333–336.
[11] C.F. Martino, P.R. Castello, Modulation of hydrogen peroxide production in cellular systems by low level magnetic fields, PLoS One 6 (8) (2011) e22753.
[12] H.T. Zhang, Z.J. Zhang, W.C. Mo, P.D. Hu, H.M. Ding, Y. Liu, Q. Hua, R.Q. He, Shielding of the geomagnetic field reduces hydrogen peroxide production in human neuroblastoma cell and inhibits the activity of CuZn superoxide dismutase, Protein Cell 8 (7) (2017) 527–537.
[13] J. Yang, J. Zhang, C. Ding, D. Dong, P. Shang, Regulation of osteoblast differentiation and iron content in MC3T3-E1 cells by static magnetic field with different intensities, Biol. Trace Elem. Res. 184 (1) (2017) 214–225.
[14] J. Zhang, X. Meng, C. Ding, L. Xie, P. Yang, P. Shang, Regulation of osteoclast differentiation by static magnetic fields, Electromagn. Biol. Med. 36 (1) (2017) 8–19.
[15] M. Wei-Chuan, L. Ying, H. Rong-Qiao, A biological perspective of the hypomagnetic field: from definition towards mechanism, Prog. Biochem. Biophys. 39 (9) (2012) 835–842.
[16] L. Vico, A. Hargens, Skeletal changes during and after spaceflight, Nat. Rev. Rheumatol. 14 (4) (2018) 229–245.
[17] D. Grimm, J. Grosse, M. Wehland, V. Mann, J.E. Reseland, A. Sundaresan, T.J. Corydon, The impact of microgravity on bone in humans, Bone 87 (2016) 44–56.
[18] R.E. Olson, H.P. Broquist, C.O. Chichester, W.J. Darby, A.C. Kolbye Jr., R.M. Stalvey, Present Knowledge in Nutrition, The Nutrition Foundation, 2012.
[19] V. Jeney, Clinical impact and cellular mechanisms of Iron overload-associated bone loss, Front. Pharmacol. 8 (2017) 77.
[20] Q. Tian, S. Wu, Z. Dai, J. Yang, J. Zheng, Q. Zheng, Y. Liu, Iron overload induced death of osteoblasts in vitro: involvement of the mitochondrial apoptotic pathway, PeerJ 4 (2016) e2611.
[21] E. Balogh, E. Tolnai, B. Nagy Jr., B. Nagy, G. Balla, J. Balla, V. Jeney, Iron overload inhibits osteogenic commitment and differentiation of mesenchymal stem cells via the induction of ferritin, Biochim. Biophys. Acta 1862 (9) (2016) 1640–1649.
[22] P. Jia, Y.J. Xu, Z.L. Zhang, K. Li, B. Li, W. Zhang, H. Yang, Ferric ion could facilitate osteoclast differentiation and bone resorption through the production of reactive oxygen species, J. Orthop. Res. 30 (11) (2012) 1843–1852.
[23] D.A. Callaway, J.X. Jiang, Reactive oxygen species and oxidative stress in osteoclastogenesis, skeletal aging and bone diseases, J. Bone Miner. Metab. 33 (4) (2015) 359–370.
[24] J. Tsay, Z. Yang, F.P. Ross, S. Cunningham-Rundles, H. Lin, R. Coleman, P. Mayer-Kuckuk, S.B. Doty, R.W. Grady, P.J. Giardina, A.L. Boskey, M.G. Vogiatzi, Bone loss caused by iron overload in a murine model: importance of oxidative stress, Blood 116 (14) (2010) 2582–2589.
[25] H.W. Lane, C.P. Alfrey, T.B. Driscoll, S.M. Smith, L.E. Nyquist, Control of red blood cell mass during spaceflight, J. Gravit. Physiol. 3 (2) (1996) 87–88.
[26] C.S. Leach, Biochemical and hematologic changes after short-term space flight, Microgravity Q. 2 (2) (1992) 69–75.
[27] S.M. Smith, S.R. Zwart, G. Block, B.L. Rice, J.E. Davis-Street, The nutritional status of astronauts is altered after long-term space flight aboard the International Space Station, J. Nutr. 135 (3) (2005) 437–443.
[28] S.R. Zwart, J.L. Morgan, S.M. Smith, Iron status and its relations with oxidative damage and bone loss during long-duration space flight on the International Space Station, Am. J. Clin. Nutr. 98 (1) (2013) 217–223.
[29] E.R. Morey-Holton, R.K. Globus, Hindlimb unloading rodent model: technical aspects, J. Appl. Physiol. (1985) 92 (4) (2002) 1367–1377.
[30] Z. Xu, W. Sun, Y. Li, S. Ling, C. Zhao, G. Zhong, D. Zhao, J. Song, H. Song, J. Li, L. You, G. Nie, Y. Chang, Y. Li, The regulation of iron metabolism by hepcidin contributes to unloading-induced bone loss, Bone 94 (2016) 152–161.
[31] T. Cavey, N. Pierre, K. Nay, C. Allain, M. Ropert, O. Loreal, F. Derbre, Simulated microgravity decreases circulating iron in rats: role of inflammation-induced hepcidin upregulation, Exp. Physiol. 102 (3) (2017) 291–298.
[32] A.R. Hargens, J. Steskal, C. Johansson, C.M. Tipton, Tissue Fluid Shift, Forelimb Loading and Tail Tension in Tailsuspended Rats, vol. 27, (1984).
[33] M.L. Bouxsein, S.K. Boyd, B.A. Christiansen, R.E. Guldberg, K.J. Jepsen, R. Muller, Guidelines for assessment of bone microstructure in rodents using micro-computed tomography, J. Bone Miner. Res. 25 (7) (2010) 1468–1486.
[34] O. Leppanen, H. Sievanen, J. Jokihaara, I. Pajamaki, T.L. Jarvinen, Three-point bending of rat femur in the mediolateral direction: introduction and validation of a novel biomechanical testing protocol, J. Bone Miner. Res. 21 (8) (2006) 1231–1237.
[35] K.J. Jepsen, M.J. Silva, D. Vashishth, X.E. Guo, M.C. van der Meulen, Establishing biomechanical mechanisms in mouse models: practical guidelines for systematically evaluating phenotypic changes in the diaphyses of long bones, J. Bone Miner. Res. 30 (6) (2015) 951–966.
[36] Y.H. An, K.L. Martinc, Handbook of Histology Methods for Bone and Cartilage, Humana Press, 2003.
[37] M.P. Nagaraja, D. Risin, The current state of bone loss research: data from spaceflight and microgravity simulators, J. Cell. Biochem. 114 (5) (2013) 1001–1008.
[38] E. Nemeth, M.S. Tuttle, J. Powelson, M.B. Vaughn, A. Donovan, D.M. Ward, T. Ganz, J. Kaplan, Hepcidin regulates cellular iron efflux by binding to ferroportin and inducing its internalization, Science 306 (5704) (2004) 2090–2093.
[39] W.C. Mo, Y. Liu, H.M. Cooper, R.Q. He, Altered development of Xenopus embryos in a hypogeomagnetic field, Bioelectromagnetics 33 (3) (2012) 238–246.
[40] E.E. Fesenko, L.M. Mezhevikina, M.A. Osipenko, R.Y. Gordon, S.S. Khutzian, Effect of the “zero” magnetic field on early embryogenesis in mice, Electromagn. Biol. Med. 29 (1–2) (2010) 1–8.
[41] W.-C. Mo, J.-P. Fu, H.-M. Ding, Y. Liu, Q. Hua, R.-Q. He, Hypomagnetic field alters circadian rhythm and increases algesia in adult male mice, Prog. Biochem. Biophys. 42 (7) (2015) 639–646.
[42] V.N. Binhi, R.M. Sarimov, Zero magnetic field effect observed in human cognitive processes, Electromagn. Biol. Med. 28 (3) (2009) 310–315.
[43] R.J. White, M. Averner, Humans in space, Nature 409 (6823) (2001) 1115–1118.
[44] S.A. Lloyd, E.R. Bandstra, J.S. Willey, S.E. Riffle, L. Tirado-Lee, G.A. Nelson, M.J. Pecaut, T.A. Bateman, Effect of proton irradiation followed by hindlimb unloading on bone in mature mice: a model of long-duration spaceflight, Bone 51 (4) (2012) 756–764.
[45] J.S. Alwood, K. Yumoto, R. Mojarrab, C.L. Limoli, E.A.C. Almeida, N.D. Searby, R.K. Globus, Heavy ion irradiation and unloading effects on mouse lumbar vertebral microarchitecture, mechanical properties and tissue stresses, Bone 47 (2) (2010) 248–255.
[46] R.D. Prisby, J.S. Alwood, B.J. Behnke, J.N. Stabley, D.J. McCullough, P. Ghosh, R.K. Globus, M.D. Delp, Effects of hindlimb unloading and ionizing radiation on skeletal muscle resistance artery vasodilation and its relation to cancellous bone in mice, J. Appl. Physiol. (1985) 120 (2) (2016) 97–106.
[47] D.A. Lipschitz, J.D. Cook, C.A. Finch, A clinical evaluation of serum ferritin as an index of iron stores, N. Engl. J. Med. 290 (22) (1974) 1213–1216.
[48] J. Daru, K. Colman, S.J. Stanworth, B. De La Salle, E.M. Wood, S.R. Pasricha, Serum ferritin as an indicator of iron status: what do we need to know? Am. J. Clin. Nutr. 106 (Suppl 6) (2017) 1634S–1639S.
[49] N.C. Andrews, Disorders of iron metabolism, N. Engl. J. Med. 341 (26) (1999) 1986–1995.
[50] G. Rishi, V.N. Subramaniam, The liver in regulation of iron homeostasis, Am. J. Physiol. Gastrointest. Liver Physiol. 313 (3) (2017) G157–G165.
[51] M. Kohyama, W. Ise, B.T. Edelson, P.R. Wilker, K. Hildner, C. Mejia, W.A. Frazier, T.L. Murphy, K.M. Murphy, Role for Spi-C in the development of red pulp macrophages and splenic iron homeostasis, Nature 457 (7227) (2009) 318–321.
[52] Y.F. He, Y. Ma, C. Gao, G.Y. Zhao, L.L. Zhang, G.F. Li, Y.Z. Pan, K. Li, Y.J. Xu, Iron overload inhibits osteoblast biological activity through oxidative stress, Biol. Trace Elem. Res. 152 (2) (2013) 292–296.
[53] C.G.T. Tahimic, R.K. Globus, Redox signaling and its impact on skeletal and vascular responses to spaceflight, Int. J. Mol. Sci. 18 (10) (2017).
[54] D. Morikawa, H. Nojiri, Y. Saita, K. Kobayashi, K. Watanabe, Y. Ozawa, M. Koike, Y. Asou, T. Takaku, K. Kaneko, T. Shimizu, Cytoplasmic reactive oxygen species and

SOD1 regulate bone mass during mechanical unloading, J. Bone Miner. Res. 28 (11) (2013) 2368–2380.
[55] L.J. Raggatt, N.C. Partridge, Cellular and molecular mechanisms of bone remodeling, J. Biol. Chem. 285 (33) (2010) 25103–25108.
[56] P. Collet, D. Uebelhart, L. Vico, L. Moro, D. Hartmann, M. Roth, C. Alexandre, Effects of 1- and 6-month spaceflight on bone mass and biochemistry in two humans, Bone 20 (6) (1997) 547–551.
[57] A. Caillot-Augusseau, M.H. Lafage-Proust, C. Soler, J. Pernod, F. Dubois, C. Alexandre, Bone formation and resorption biological markers in cosmonauts during and after a 180-day space flight (Euromir 95), Clin. Chem. 44 (3) (1998) 578–585.
[58] P. Cabahug-Zuckerman, D. Frikha-Benayed, R.J. Majeska, A. Tuthill, S. Yakar, S. Judex, M.B. Schaffler, Osteocyte apoptosis caused by hindlimb unloading is required to trigger osteocyte RANKL production and subsequent resorption of cortical and trabecular bone in mice femurs, J. Bone Miner. Res. 31 (7) (2016) 1356–1365.
[59] J.I. Aguirre, L.I. Plotkin, S.A. Stewart, R.S. Weinstein, A.M. Parfitt, S.C. Manolagas, T. Bellido, Osteocyte apoptosis is induced by weightlessness in mice and precedes osteoclast recruitment and bone loss, J. Bone Miner. Res. 21 (4) (2006) 605–615.
[60] W. Xie, S. Lorenz, S. Dolder, W. Hofstetter, Extracellular iron is a modulator of the differentiation of osteoclast lineage cells, Calcif. Tissue Int. 98 (3) (2016) 275–283.